J. Synchrotron Rad. (1997). **4**, 223–227

Investigation of the Variation in Orientation and Crystallinity in Poly(ethylene terephthalate) Containers Using Microfocus X-ray Diffraction

C. Martin,[a] A. Mahendrasingam,[a] W. Fuller,[a] J. L. Harvie,[b] D. J. Blundell,[c] J. Whitehead,[c] R. J. Oldman,[c] C. Riekel[d] and P. Engström[d]

[a]*Department of Physics, Keele University, Keele, Staffordshire ST5 5BG, UK,* [b]*ICI Polyesters, PO Box 90, Wilton, Middlesbrough, Cleveland TS90 8JE, UK,* [c]*ICI Wilton Research and Technology Centre, PO Box 90, Wilton, Middlesbrough, Cleveland TS90 8JE, UK, and* [d]*ESRF, BP 220, F-38043 Grenoble CEDEX, France. E-mail: pha40@keele.ac.uk*

(*Received 6 February 1997; accepted 20 March 1997*)

The microfocus X-ray beamline at the European Synchrotron Radiation Facility has been used to investigate the variation in molecular orientation and crystallinity in the wall of a container fabricated from poly(ethylene terephthalate). Two-dimensional wide-angle X-ray scattering patterns were recorded and displayed in real time as the specimen was tracked across the incident X-ray beam enabling the measurement of textural changes to be made with a spatial resolution of $\sim 2\,\mu$m.

Keywords: PET; X-ray diffraction; microfocus; orientation; crystallinity; wide-angle scattering; CCD detectors.

1. Introduction

We have recently reported the use of microfocus instrumentation on beamline ID13 at the European Synchrotron Radiation Facility to investigate the variation in polymer orientation and crystallinity in spherulites of the optically active thermoplastic homopolymer poly-D-(−)-3-hydroxybutyrate (Mahendrasingam *et al.*, 1995). In these studies the diameter of the X-ray beam at the specimen was $\sim 10\,\mu$m and this spatial resolution was sufficient to show that the crystallites in the specimen were systematically oriented so that the *a* axis in each crystallite was oriented parallel to a radius of the spherulite but with the degree of orientation and crystallinity decreasing towards the centre of the spherulite. Using similar techniques, local variations in polymer chain orientation have been described in injection-moulded liquid-crystalline polymers (Dreher, Zachmann, Riekel & Engström, 1995).

Physical properties, such as strength and gas-transport properties, of artefacts fabricated from poly(ethylene terephthalate) (PET) depend on the degree of polymer orientation and crystallinity and its variation in the artefact. In an effort to improve the efficiency and quality control in the processing of bulk polymers in the manufacture of products such as containers from PET (which have a high performance specification), we have undertaken a preliminary study of the dependence of polymer orientation and crystallinity on fabrication conditions. This report describes experiments where the microscopic variation of these characteristics is studied with a resolution of $\sim 2\,\mu$m within the wall of such a container.

The manufacture of PET containers involves first the injection moulding of an unoriented amorphous preform followed by blowing the preform into a cold shaped mould to form the container. Often this process is carried out *via* a two-stage route in which the preform is first cooled to room temperature and is then subsequently reheated for the blowing stage. However, the container used for this investigation was formed by the alternate one-stage route where the hot preform is moved to a conditioning zone in order to cool to the blowing temperature before moving to the blowing zone. In both these manufacturing routes there is a significant variation in the temperature profile through the wall of the preform at the moment of extension in the blowing zone. During blowing, the inner surface of the preform is cooled by the expansion of the compressed air used for inflation, the outer surface is cooled by contact with the (relatively) cold mould whilst the internal thermal energy is raised by strain heating. In addition, the contour shape of the container and the complex blowing process itself produces considerable variation in wall thickness and direction of stretching at different positions in the container. The polymer therefore experiences a wide variation in draw temperature, draw ratio and draw direction at different positions of the container and at different depths in the wall, resulting in a wide variation of orientation and crystallinity in the local polymer structure. In order to understand the mechanical properties of the container it is necessary to be able to characterize how this structure can vary. One of the main difficulties of this characterization, and the reason for undertaking this investigation, is the difficulty of probing variations in structure through the container wall

with sufficient spatial resolution and thus in establishing the connections between local properties and the manufacturing process.

2. Experimental techniques

In the investigations on poly-D-(–)-3-hydroxybutyrate previously described, a 10 μm-diameter Rigaku post-collimator was used (7 μm-diameter FWHM), resulting in a photon flux density at the sample of $\sim 5 \times 10^7$ photons s^{-1} μm^{-2} mA^{-1} at a wavelength of 0.92 Å (Engström, Fiedler & Riekel, 1995). In this study, tapered glass capillary focusing optics (Bilderback, Thiel, Pahl & Brister, 1994) were used in place of the collimator, providing an increase in flux density by a factor of about four, whilst reducing the full beam size to 2.3 μm diameter at the exit of the capillary, although with a beam divergence of ~3 mrad (Engström, Riekel & Chanzy, 1995).

Crucial to the experiments described here was the availability of a computer-controlled Physik Instrumente *X/Y* stage (which allowed the specimen to be tracked in two dimensions perpendicular to the X-ray beam with a spatial resolution of ~0.1 μm) and a Photonic Science CCD X-ray detector with a sensitive area of 92 × 69 mm and an effective pixel area of ~120 × 120 μm. The specimen-to-detector distance was approximately 6 cm and at this distance diffraction data could be recorded for *d* spacings from 15 to 1.5 Å. Diffraction patterns were recorded with an exposure time of 40 ms, integrated over 500 frames and digitized using a Synoptics i860-based framegrabber (Mahendrasingam *et al.*, 1995). Simultaneously, the data were recorded 'live' on a standard VCR using VHS format, which introduced the possibility of post-experimental re-digitization. Whilst data recorded on video tape have limitations for use in a detailed X-ray structural refinement, they are more than adequate for the determination of molecular orientation and crystallinity. The linear step size between data points was 30 μm, resulting in a total of 32 data points across the full width of the sample.

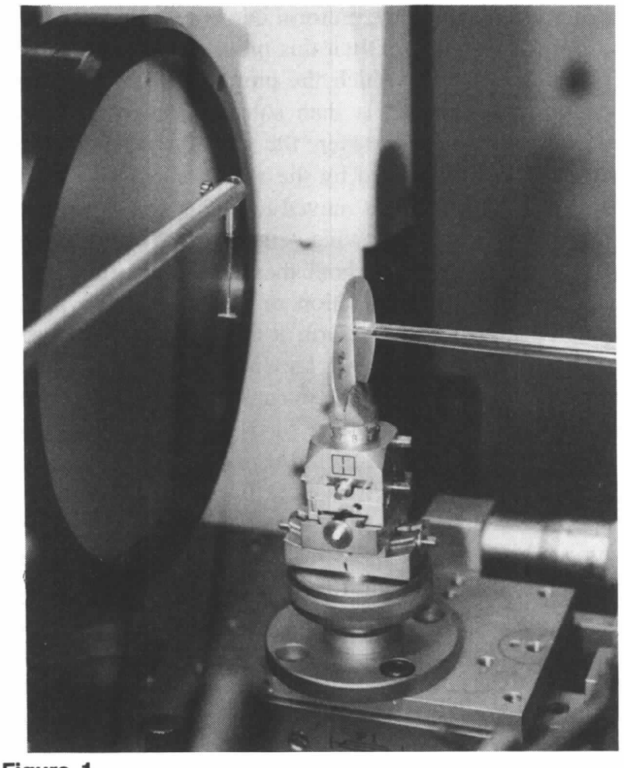

Figure 1
Photograph of a thin-sectioned specimen in its epoxy resin support disc mounted on a goniometer on the *X/Y* stage on ID13. Centre right is seen the glass capillary, whilst to the left of the specimen are the suspended lead beamstop and the Photonic Science CCD detector.

The PET container used for this study was a nominal 24 oz (approximately 675 g) conical jar that had been manufactured using a one-stage Aoki machine. The sample was taken from near the top of the conical wall where the wall thickness was ~1 mm. The expectation from the manufacturing process is that the temperature inside the wall of the preform would have been hotter than either of the outside faces at the moment of blowing.

The sample for the microbeam X-ray examination was prepared by first cutting a 10 mm-square piece from the container and then embedding it in epoxy resin. The embedded block was mounted on a Metals Research Microslice 2 fitted with a 50 μm-thick diamond-tipped annular saw. The block was positioned so that the plane of the saw was perpendicular to the sample wall and parallel to the longitudinal direction of the container. Two successive cuts were made with the saw so as to produce a slice approximately 90 μm thick.

Fig. 1 shows a specimen mounted on the *X/Y* stage with its orientation with respect to the incident X-ray beam illustrated.

3. Results

Fig. 2 shows selected frames from the longitudinally sliced samples taken from a dataset comprising 32 frames. The patterns show a marked variation in crystallinity through the thickness of the wall at this point. Particularly at the inside edge there are strong oriented crystalline reflections superimposed on a fairly isotropic amorphous halo. The intensification of the crystal reflections around the equator is consistent with preferential chain alignment along the longitudinal axis of the jar. The intensity of the crystal reflections diminishes towards the centre of the wall thickness leaving an almost isotropic amorphous diffraction halo. Nearer the outer edge of the wall there is an intensification of the halo on the equator indicating an increasing degree of orientation in the disordered chains. The oriented crystalline pattern is not that normally seen from highly oriented PET fibres. The strongest features in the full diffraction pattern are the (100) and (1$\bar{1}$0) reflections and there is an absence of any (010) reflections near the equator. This would be consistent with chain alignment in the longitudinal axis but with a preference for the (100) crystal planes to lie parallel to the plane of the bottle wall. This alignment feature of

(100) planes is a common feature in oriented PET films (Salem, 1992; Casey, 1977; Bower, Jarvis & Ward, 1986). Another unusual feature is that the (100) reflections are split each side of the equator indicating a systematic tilting of the crystalline chains away from the longitudinal axis. This feature was reported in the original crystal structure analysis and was found to occur when fibre samples were annealed at higher temperatures (Daubeny, Bunn & Brown, 1954).

A detailed analysis was conducted on the data using a customized suite of computer programs and routines. Corrections were applied for detector dark current, variations in sample thickness, for the amorphous diffraction due to the glass capillary and for air scatter. Radial and azimuthal scans were made through appropriate reflections in order to monitor crystallinity and orientation by automated fitting of Gaussian profiles to the resultant one-dimensional data files.

Fig. 3 shows the variation in successive diffraction patterns of a radial scan through the peak intensity of the (100) reflection (close to the equator). The procedure employed to fit functions to these radial scans is illustrated in Fig. 4. Here, the 'unoriented background' (up to s = 0.41 Å^{-1}, where s is the radial scattering vector $2 \sin \theta/\lambda = 1/d$) was determined from the scattering along the meridian. The 'oriented background' was of the same form but was linearly scaled and was included as a fit variable. Finally, two Gaussian functions representing the scattering contributions from the (100) and (1$\bar{1}$0) crystallographic planes were included in the fitting routine where only the radial position of the peaks was not allowed to vary. The starting parameters for each frame were identical and the fitting routine was executed automatically on the complete dataset. Subsequently, from the results for the (100) reflection, the Scherrer relation was used to provide an estimate of relative crystallite size (Klug & Alexander, 1974), and since corrections were not made for smearing due to the highly divergent incident beam they provide a lower limit for crystallite size. The area under the same peak was used as an indication of relative crystallinity. In Fig. 5 the variation in relative crystallite size and relative crystallinity calculated by these methods are plotted as a function of position in the sample.

Fig. 6 shows the azimuthal scans through the (1$\bar{1}$0) reflection. The components included in the fitting routine for these data are illustrated in Fig. 7, where the background has been modelled by a linear function through π radians. The form of the 'tails' of the reflection [due to the overlapping (100) reflections] was modelled by a pair of Gaussian functions. In Fig. 8 the result of analyzing the scans using expressions for orientation derived by Lovell & Mitchell (1981) is presented and it should be noted that the orientation function $\langle P_{2n}(\cos a)\rangle$ described here is a composite of orientation effects.

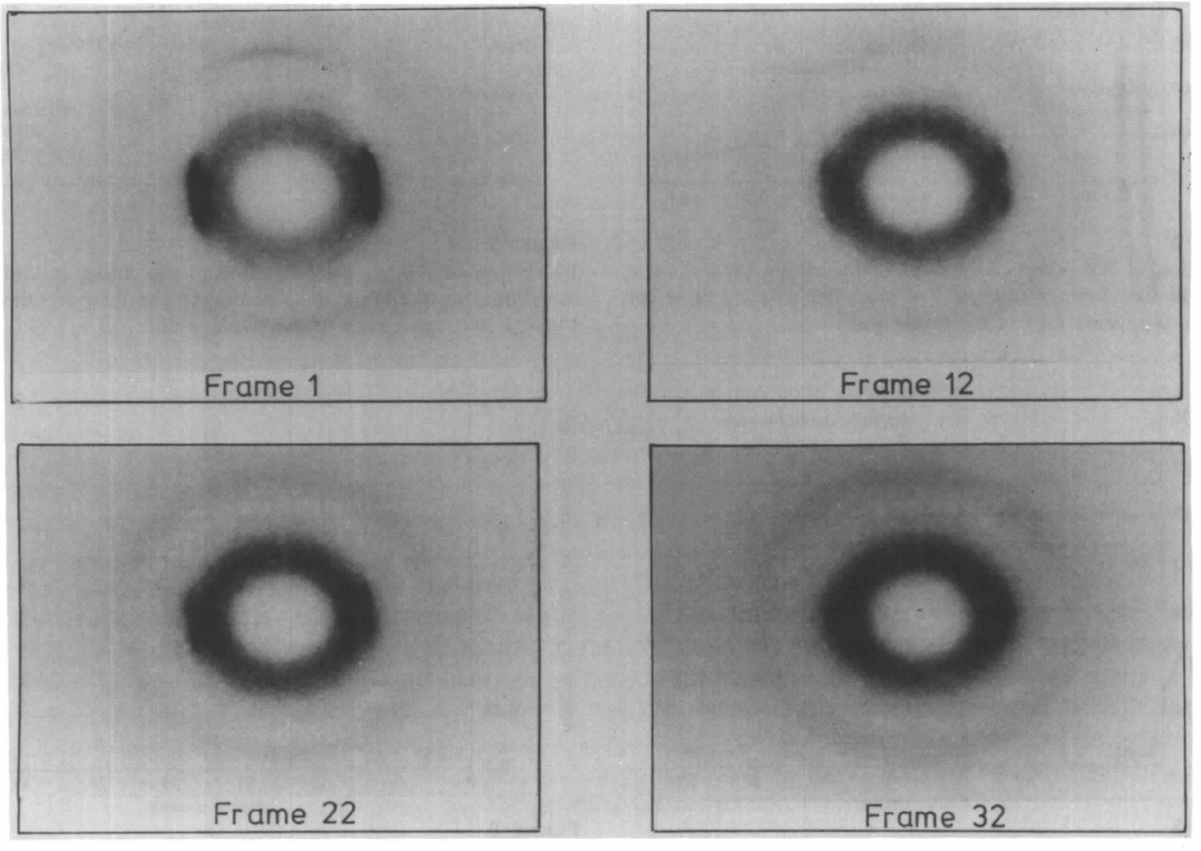

Figure 2
X-ray diffraction patterns selected from the 32 frames recorded during the experiment. Frame 1 was collected at the inside face of the bottle wall, whilst frame 32 was collected at the outside face.

In this data analysis the initial observations of the full diffraction patterns were confirmed and extended and the temperature-dependent effects on crystallinity and orientation are clearly demonstrated in Figs. 5 and 8. The general trends can be rationalized in terms of a variation in temperature across the wall thickness at the moment of extension. At the outer edge of the wall, where the temperature is lowest, the degree of extension has produced

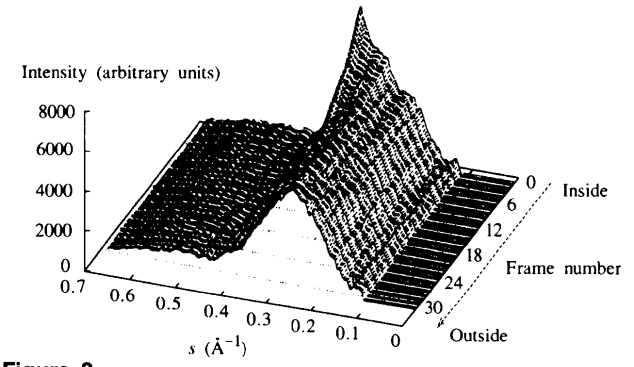

Figure 3
Quasi three-dimensional plot showing the variation of diffracted intensity of a radial scan through the peak intensity of the (100) reflection as a function of position in the sample.

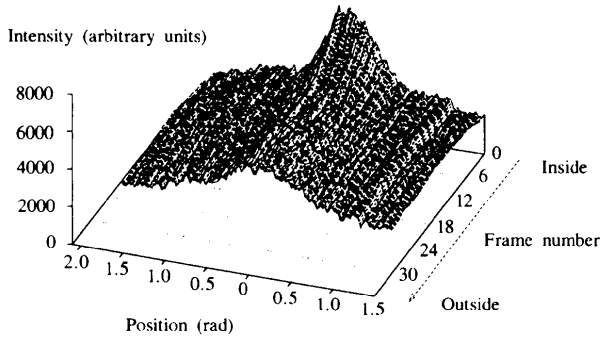

Figure 6
Quasi three-dimensional plot showing the variation of diffracted intensity of an azimuthal scan through the peak intensity of the $(1\bar{1}0)$ reflection as a function of position in the sample.

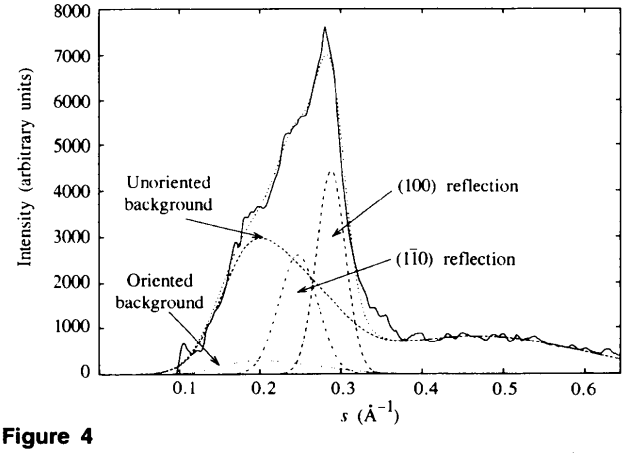

Figure 4
Illustration of the components used in the fitting procedure to determine the variation in crystallite size. The data are those for frame 1, the inside face of the bottle wall.

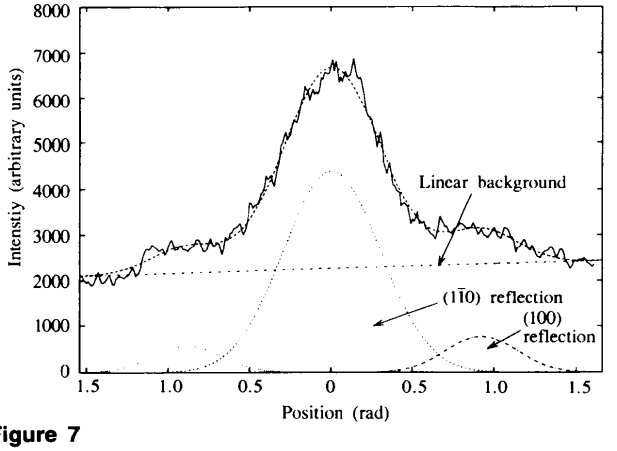

Figure 7
Illustration of the components used in the fitting procedure to determine the variation in orientation. The data are those for frame 1, the inside face of the bottle wall.

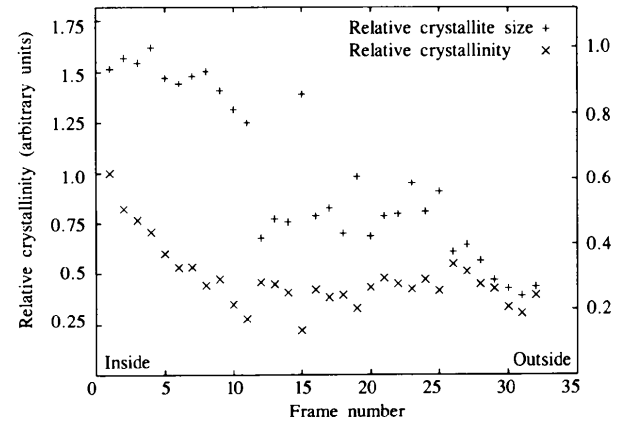

Figure 5
Variation of relative crystallite size and relative crystallinity as a function of position in the sample obtained by curve fitting the scans of Fig. 3.

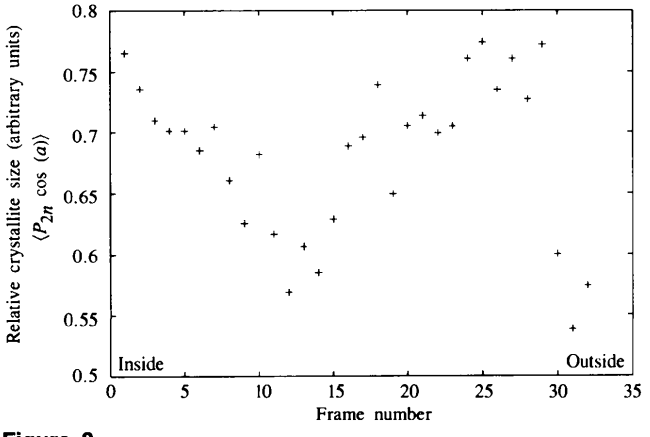

Figure 8
Variation of the (composite) orientation function $\langle P_{2n}(\cos a)\rangle$ as a function of position in the sample obtained by curve fitting the scans of Fig. 6.

a degree of orientation in the disordered chains but not enough orientation to enable them to crystallize. Towards the centre the higher temperature has allowed a degree of relaxation in the orientation of the amorphous chains. On the inside edge there is a long enough residence at a higher temperature to enable crystallinity to develop from the partially oriented amorphous matrix.

4. Conclusions

These studies demonstrate that an intense micrometre-sized X-ray beam can be used to investigate local textural variations in technologically important artefacts fabricated from polymer materials. The specimens from PET vessels studied in this work exhibited clear variation in polymer orientation, crystallite size and crystallinity over the $\sim$1000 μm thickness of the wall with significant variation occurring over distances of the order of $\sim$50 μm. While this variation is on a coarser distance scale than that which could be observed with an X-ray incident beam size as small as that available on Beamline ID13, confidence in the experimental and analytical methods employed is gained by the fact that the small beam size compared with the step size means that each diffraction image is essentially an independent measurement and has resulted in the establishment of systematic and sensible variations. Confidence is also added to the future application of these procedures in the investigation of structures where polymer orientation and crystallinity can be expected to vary over distances as small as a few micrometres, *e.g.* at interfaces in laminated materials.

We plan a series of experiments where the scope of the present work is extended by investigating variations in crystallinity and orientation in samples taken from different positions and both in the longitudinal and circumferential directions in PET containers and where interfaces in laminated materials are studied.

This work was supported by SERC grants GR/J/01950 and GR/H/67966 and benefited from exploratory studies on beamline ID13 supported by SERC grant GRJJ/57797 to V. T. Forsyth, AM and WF and from further allocations of beam time by the ESRF. Much of the equipment used in this study was assembled and commissioned in the Keele Physics Department. We are grateful to M. Daniels, M. G. Davies, D. M. Evans, J. Gorini, E. J. T. Greasley, G. Marsh, H. E. Moors, M. P. Wallace and P. Wattecamps for technical support and help with preparation of the manuscript.

References

Bilderback, D. H., Thiel, D. J., Pahl, R. & Brister, K. E. (1994). *J. Synchrotron Rad.* **1**, 37–42.

Bower, D. I., Jarvis, D. A. & Ward, I. M. (1986). *J. Polym. Sci.* B**24**, 1459–1479.

Casey, M. (1977). *Polymer*, **18**, 1219–1226.

Daubeny, R. de P., Bunn, C. W. & Brown, C. J. (1954). *Proc. R. Soc. London Ser. A*, **226**, 531–542.

Dreher, S., Zachmann, H. G., Riekel, C. & Engström, P. (1995). *Macromolecules*, **28**, 7071–7074.

Engström, P., Fiedler, S. & Riekel, C. (1995). *Rev. Sci. Instrum.* **66**, 1348–1350.

Engström, P., Riekel, C. & Chanzy, H. (1995). *ESRF Newsl.* **24**, 8–9.

Klug, H. P. & Alexander, L. E. (1974). *X-ray Diffraction Procedures for Polycrystalline and Amorphous Materials*, 2nd ed., pp. 687–690. New York: Wiley–Interscience.

Lovell, R. & Mitchell, G. R. (1981). *Acta Cryst.* A**37**, 135–137.

Mahendrasingam, A., Martin, C., Fuller, W., Blundell, D. J., MacKerron, D. H., Rule, R. J., Oldman, R. J., Liggat, J., Riekel, C. & Engström, P. (1995). *J. Synchrotron Rad.* **2**, 308–311.

Salem, D. R. (1992). *Polymer*, **33**, 3182–3188.